***Science* Supporting Online Material**

Intracellular Parasite Invasion Strategies

L. D. Sibley
doi:10.1126/science.1094717

Science Supporting Online Material
SOM Text
Fig. S1 to S11
References
Movies S1 to S10

Cytoskeletal Organization

The phylum Apicomplexa (*S1*, *S2*) is defined by its apical specialization and complex cytoskeleton. The cell cortex is comprised of several membranous layers and the underlying cytoskeleton. The arrangement of these layers is shown for *Toxoplasma gondii* as a representative example (Fig. S1). Starting from the innermost layer, a rigid cell shape is imparted by a system of subpellicular microtubules that are collected at the anterior end by a unique organizing center called the conoid (*S3*). Extending over the microtubules is a complex meshwork of filaments, composed in part of the proteins IMC1 and IMC2 (*S4*). The cell membrane consists of an outer plasma membrane underlain by a double, flattened membrane called the inner membrane complex (IMC). Freeze-fracture studies have revealed that the IMC contains numerous inner membrane particles that presumably represent proteins embedded within the membrane (*S5*, *S6*).

Fig. S1. Graphic depiction of the layers of *Toxoplasma gondii* seen in cut-away view. (**A**) The conoid is revealed by transmission EM after detergent extraction and negative staining as described previously [image used with permission (*S6*)]. (**B**) Encasing the microtubules is a meshwork of filaments observed by transmission EM after detergent extraction and platinum freeze-dried replica formation (image provided by Robin Roth and John Heuser, Washington University). The plasma membrane of the parasite is underlain by the inner membrane complex. (**C**) Freeze-etch replicas of this layer reveal that the IMC is comprised of two flattened cisternae that contain numerous inner membranous particles embedded in the membrane [image used with permission (*S6*)]. Graphic image was generated by Paul W. Warfel with assistance of Naomi Morrissette.

Figure S1

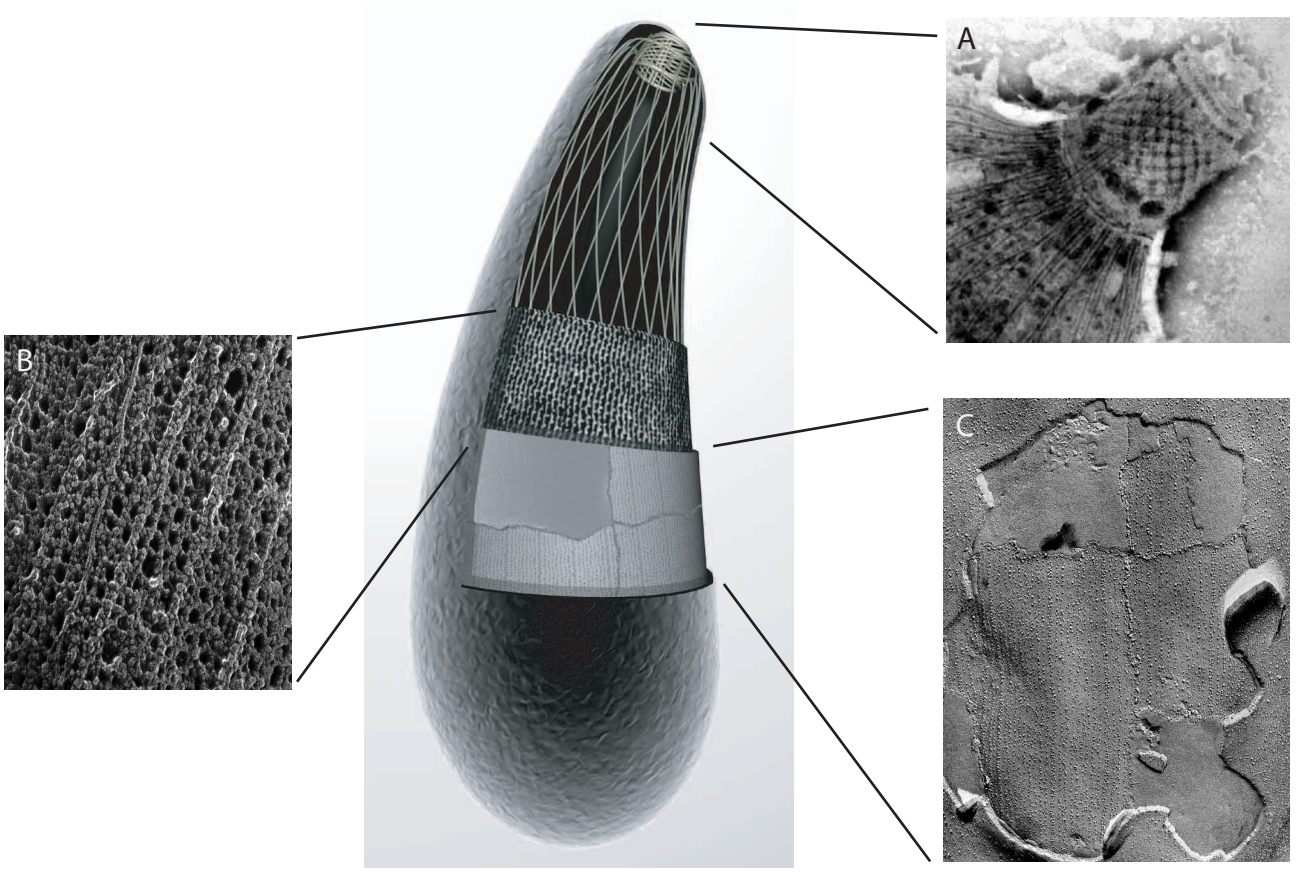

Gliding Motility

Apicomplexan parasites display a conserved behavior of substrate-dependent motility termed "gliding" (*S7*, *S8*). Apicomplexans are generally slender, crescent-shaped cells that range in size from 4 to 9 microns long by 1 to 3 microns wide. The following video images depict gliding motility as it occurs in vitro by a variety of apicomplexans.

Toxoplasma

Movies depicting gliding motility by *Toxoplasma gondii* tachyzoites were recorded by Sebastian Håkannson (Washington University) as described previously (*S9*). Videos are projected at twice normal speed. During circular gliding (Movie S1), the parasite traces a circular pattern, moving counterclockwise (when viewed from above) while lying on its right side (the convex side being defined as dorsal). Helical gliding (Movie S2) occurs in a clockwise manner and involves rotation about the long axis of the cell. During helical gliding, the parasite traces out an arc along the dorsal surface of the cell. Helical gliding involves two different phases as described previously (*S9*). During the first 180^{o} rotation, the parasite moves forward one body length. It then flips from the right side to the left side in a rapid motion that does not result in net forward movement. The successive rotational movements trace out a roughly linear pattern across the substrate. Note that only helical gliding leads to cell entry (*S9*).

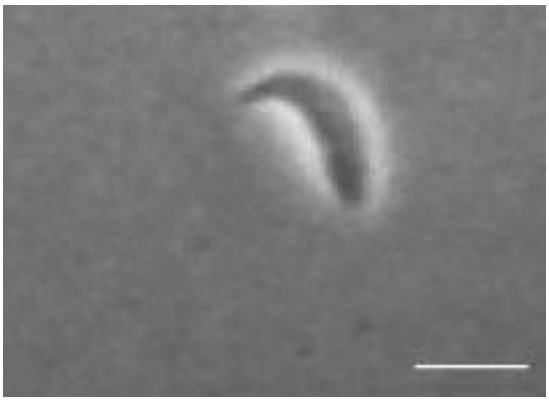

Fig. S2. Still from Movie S1. Circular gliding by *T. gondii* tachyzoites. Scale bar = 5 microns.

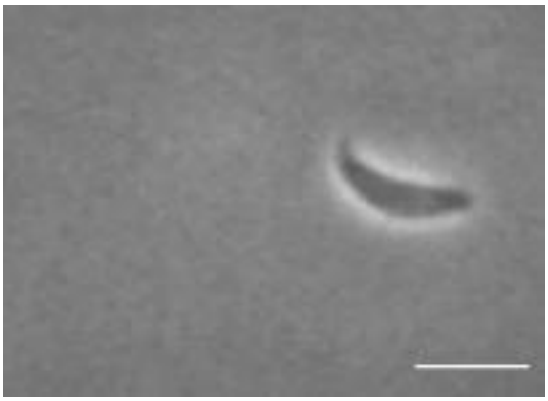

Fig. S3. Still from Movie S2. Helical gliding by *T. gondii* tachyzoites. Scale bar = 5 microns.

Cryptosporidium

Movies depicting gliding motility by *Cryptosporidium parvum* sporozoites were recorded by Dawn Wetzel (Washington University) with assistance from Joanne Schmidt (University of Illinois) as described previously (*S10*). Movies are projected at 1× original speed. Gliding motility by *Cryptosporidium* is analogous to that described above in *Toxoplasma*. The parasite moves in either circular (Movie S3) or helical patterns (Movie S4). Helical gliding traces a more undulating path than that of *Toxoplasma*. This difference may reflect the fact that *Cryptosporidium* sporozoites are more slender. Moreover, sporozoite gliding is significantly faster than that by *Toxoplasma* tachyzoites. *Cryptosporidium* gliding results in the deposit of trails on the substrate (*S11*), similar to *Toxoplasma* (*S9*).

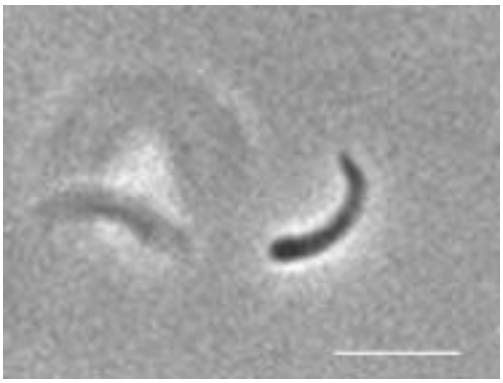

Fig. S4. Still from Movie S3. Circular gliding by *C. parvum* sporozoites. Scale bar = 5 microns.

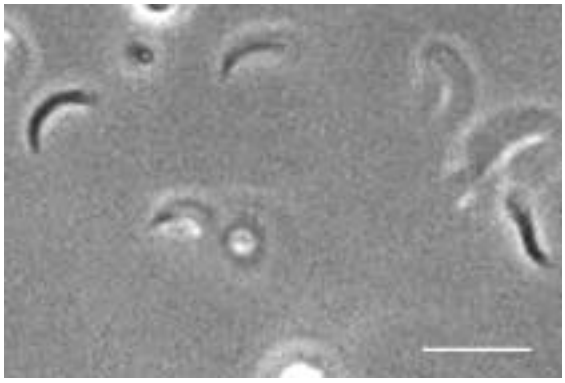

Fig. S5. Still from Movie S4. Helical gliding by *C. parvum* sporozoites. Scale bar = 5 microns.

Plasmodium

Plasmodium sporozoites also display gliding motility on solid substrates. Gliding is characterized by circular patterns (Movie S5) that result in deposits of trails on the substrate (*S12*). *Plasmodium* sporozoites also undergo undulating helical gliding, as described previously (*S13*) and depicted in Movie S6. During helical gliding, the parasite adopts a more accentuated bend in the middle of the cell body compared with that of *Toxoplasma*, and this pattern is also seen in *Cryptosporidium* (Movie S4). As in the case of *Toxoplasma*, helical gliding precedes cell invasion by malaria sporozoites (Movie S7).

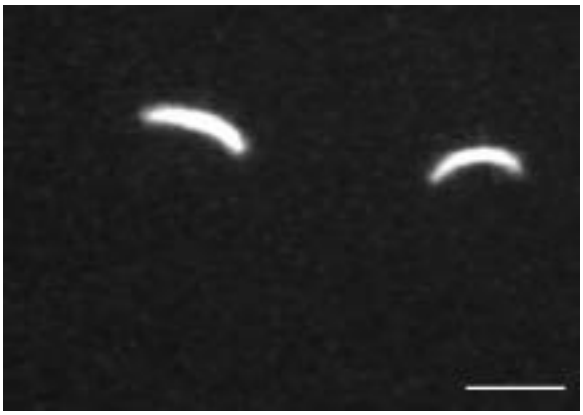

Fig. S6. Still from Movie S5. Circular gliding of *P. berghei* sporozoites. Provided by J. Dvorak and M. Akaki (NIH). Elapsed time shown in movie. Scale bar = 10 microns.

Fig. S7. Still from Movie S6. Helical gliding of *P. berghei* sporozoites. Provided by J. Vanderberg (NYU). Elapsed time shown. Scale bar = 10 microns.

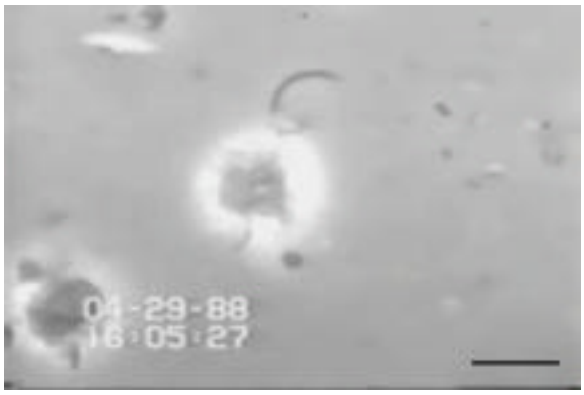

Fig. S8. Still from Movie S7. Helical gliding by *P. bergehi* sporozoites proceeds invasion of macrophage *in vitro*. Provided by J. Vanderberg (NYU). Elapsed time shown. Scale bar = 10 microns.

During development in the insect, the ookinete form also displays gliding motility (Movie S8). Ookinetes develop from the zygote after fertilization occurs in the mosquito midgut lumen after a blood meal. The ookinete penetrates the midgut epithelium, crossing this barrier to develop into an oocyst on the basolateral surface. Passage of the parasite across the epithelium inflicts damage on the epithelium and leads to cell death (*S14*, *S15*).

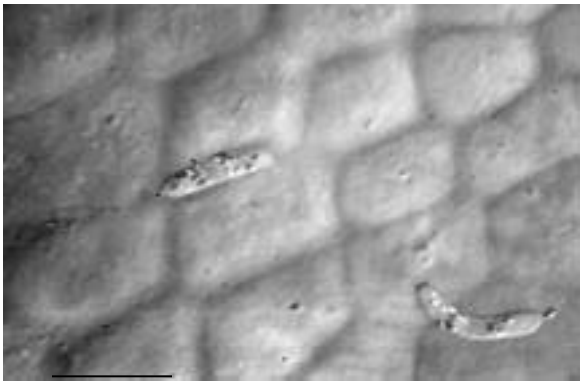

Fig. S9. Still from Movie S8. Gliding motility of *P. berghei* ookinetes on insect midgut epithelial cells. Gliding occurs across the surface of the cells, invasion occurs along the lateral edge from the apical surface. Provided by J. Dvorak (NIH). Scale bar = 10 microns.

Gregarina

Gregarines are enteric parasites of invertebrates. They are grouped in the Apicomplexa based on their life cycle features and conserved SSU sequences, which reveal they are most closely aligned with *Cryptosporidium* (*S16*, *S17*). The images shown here represent *Gregarina polymorpha* that were recovered from the flour beetle (*Tenebrio moilitor*). Gliding on the substrate results in gradual forward movement (left to right in Movie S9). A similar mechanism results in translocation of 10-micron beads along the surface, resulting in accumulation at the posterior end of the cell (top in Movie S10). *Gregarina* movies are projected at 1× normal speed. Motility of gregarines is further described in (*S7*, *S8*, *S18*).

Fig. S10. Still from Movie S9. Gliding motility by *G. polymorpha*. Provided by C. King (University College, London). Scale bar = 20 microns.

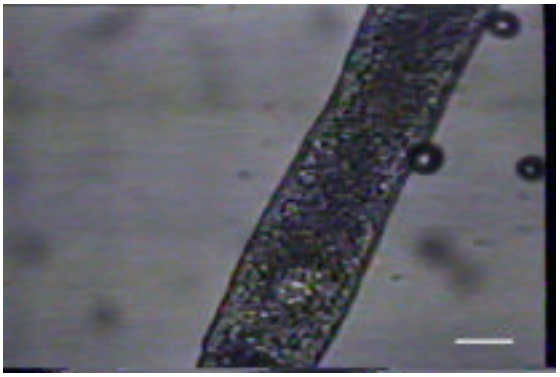

Fig. S11. Still from Movie S10. Translocation of beads among the surface of *G. polymorpha*. Provided by C. King (University College, London). Scale bar = 20 microns.

References

S1. N. S. Morrissette, L. D. Sibley, *Microbiol. Mol. Biol. Rev* .**66**, 21 (2002).

S2. B. Nichols, M. Chiappino, *J. Protozool.* **34**, 217 (1987).

S3. K. Hu, D. S. Roos, J. M. Murray, *J . Cell Biol.* **156**, 1039 (2002).

S4. T. Mann, C. Beckers, *Mol. Biochem. Parasitol.* **115**, 257 (2001).

S5. E. Ferreira, J. F. Dubremetz, *J. Protozool.* **29**, 304 (1982).

S6. N. S. Morrissette, J. M. Murray, D. S. Roos, *J. Cell Sci.* **110**, 35 (1997).

S7. C. A. King, Parasitol. *Today* **11**, 315 (1988).

S8. T. M. Preston, C. A. King, *Acta Protozoologica* **35**, 3 (1996).

S9. S. Håkansson, , H. Morisaki, J. E. Heuser, L. D. Sibley, *Mol. Biol. Cell* **10**, 3539 (1999).

S10. D. M. Wetzel, S. Håkansson, K. Hu, D. S. Roos, L. D. Sibley, *Mol. Biol. Cell* **14**, 396 (2003).

S11. M. J. Arrowood, C. R. Sterling, M. C. Healey, *J. Parasitol.* **77**, 315 (1991).

S12. M. J. Stewart, J. P. Vanderberg, *J. Protozool.* **35**, 389 (1988).

S13. J.P. Vanderberg, S. Chew, M. J. Stewart, *J. Protozool.* **37**, 528 (1990)

S14. Y. S. Han, J. K. Thompson, F. C. Kafatos, C. Barillas-Mury, *EMBO J.* **19**, 6030 (2000).

S15. H. Zieler, J. A. Dvorakk, *Proc. Natl. Acad. Sci. U.S.A.* **97**, 11516 (2000).

S16. J. R. Barta, *Vet. Parasitol.* **101**, 175 (2001).

S17. R. A. Carreno, D. S. Martin, J. R. Barta, *Parasitol. Res.* **85**, 899 (1999).

S18. C. A. King, *Cell Biol. Intl. Rep.* **5**, 297 (1981).